Self-Similar Structure in Goldbach Deviations: L-Function Zeros and the Twin Prime Signature

Ruqing Chen

GUT Geoservice Inc., Montreal

ruqing@hotmail.com

Repository: `https://github.com/Ruqing1963/goldbach-fractal-analysis`

January 2026

Abstract

We use the Goldbach representation function as a testbed to study arithmetic structure in number-theoretic error terms. We present numerical evidence suggesting that the deviation from the Hardy-Littlewood formula exhibits nontrivial arithmetic structure consistent with a *constant consistency principle*: the twin prime constant $C_2 \approx 0.6602$ appears in both the main term amplitude and the fluctuation envelope. Spectral analysis in the logarithmic domain reveals oscillatory components consistent with known Dirichlet L-function zeros within the available FFT resolution ($\Delta\gamma \approx 1.25$). Hurst exponent analysis yields $H = 0.85 \pm 0.02$ after detrending, significantly exceeding the corresponding null baseline; the quoted significance refers to deviation from the specific Poisson–Hardy–Littlewood null model. We propose a conjectural correction formula for Goldbach counts incorporating these structural terms, and discuss the transferability of these methods to other additive problems.

Keywords: Goldbach conjecture, Hardy-Littlewood formula, Dirichlet L-functions, Riemann zeros, fractal analysis, twin prime constant, self-similarity, scale invariance

Notation

Symbol	Definition
$G(N)$	Number of representations of N as sum of two primes
$\mathrm{HL}(N)$	Hardy-Littlewood prediction $2C_2S(N)\mathrm{Li}_2(N)$
C_2	Twin prime constant $\prod_{p>2}(1-(p-1)^{-2}) \approx 0.6601618$
$S(N)$	Singular series for N
χ_p	Legendre symbol modulo prime p
$c_p(N)$	Dirichlet coefficient: amplitude of χ_p contribution to $\delta(N)$
κ	Universal amplitude in decay law $c_p(N) \sim \kappa/(\varphi(p)\ln N)$
γ	Imaginary part of L-function zero $\rho = \frac{1}{2} + i\gamma$
H	Hurst exponent quantifying long-range dependence

1 Introduction

The Goldbach conjecture—that every even integer greater than two equals a sum of two primes—provides an ideal testbed for studying arithmetic structure in additive number theory. While a proof remains elusive, the Hardy-Littlewood asymptotic formula

$$G(N) \sim 2C_2S(N)\mathrm{Li}_2(N) \tag{1}$$

captures the dominant behavior, leaving the error term as an object of independent interest [Hardy and Littlewood, 1923]. This paper develops methods for analyzing such error terms that may transfer to other additive problems.

1.1 Context: Papers I–IV

Our previous work established:

- **Paper I** [Chen, 2026a]: Validation of Hardy-Littlewood to $N = 10^{12}$; correlation between $G(N) - \mathrm{HL}(N)$ and Dirichlet characters $\chi_p(N)$.
- **Papers II–III** [Chen, 2026b,c]: Crossover phenomenon; spectral rigidity and sub-Poissonian statistics.
- **Paper IV** [Chen, 2026d]: Discovery of the second main term; measurement $\kappa = 0.70 \pm 0.04$ from $N \in [10^5, 2 \times 10^8]$.

1.2 Main Contributions of Paper V

This paper addresses: *Why does $\kappa \approx C_2$?* We provide:

1. A formal conjecture (Conjecture 2.3) stating the constant consistency principle.
2. Spectral analysis via "Riemann Radar" showing peaks consistent with L-function zeros within FFT resolution (Table 1).
3. Null hypothesis test indicating arithmetic origin of long-range persistence relative to a specific null model.
4. A conjectural Chen–Goldbach correction formula supported by numerical evidence (Conjecture 6.1).

2 The Constant Consistency Principle

2.1 Dirichlet Decomposition

The normalized deviation

$$\delta(N) = \frac{G(N) - \mathrm{HL}(N)}{\mathrm{HL}(N)} \tag{2}$$

admits the decomposition

$$\delta(N) = \sum_{p \in \mathcal{P}} c_p(N)\chi_p(N) + \epsilon(N), \tag{3}$$

where $\mathcal{P} = \{3, 5, 7, 11, \ldots\}$ and $|\epsilon(N)| = O(1/\ln^2 N)$.

Definition 2.1 (Dirichlet Coefficients)**.** For each prime p, the *Dirichlet coefficient* $c_p(N)$ is the amplitude of the χ_p contribution to $\delta(N)$, extracted via regression over residue classes modulo p.

2.2 The Universal Decay Law

Numerical analysis reveals:

$$c_p(N) = \frac{\kappa}{\varphi(p)\ln N} + O\left(\frac{1}{\ln^2 N}\right), \tag{4}$$

with κ independent of p. Global regression yields:

$$\kappa = 0.70 \pm 0.04, \quad \frac{\kappa}{C_2} = 1.06 \pm 0.06. \tag{5}$$

Remark 2.2 (Statistical Consistency with $\kappa = C_2$). The observed ratio $\kappa/C_2 = 1.06$ deviates from unity by 0.06, which is exactly 1σ given the uncertainty ± 0.06. A formal hypothesis test[1]:

- H_0: $\kappa = C_2$ (i.e., $\kappa/C_2 = 1$)
- H_1: $\kappa \neq C_2$
- Test statistic: $z = (1.06 - 1.00)/0.06 = 1.0$
- Two-tailed p-value: $p = 0.32$

We **cannot reject** H_0 at any conventional significance level ($\alpha = 0.05, 0.01$). The slight deviation from unity may be attributed to finite-range effects: at $N \leq 1.5 \times 10^6$, higher-order terms of order $O(1/\ln^2 N)$ have not yet fully decayed. Data from Chen [2026d] extending to $N = 2 \times 10^8$ yielded κ/C_2 closer to unity, consistent with asymptotic convergence.

[1]The p-value is computed via a standard two-tailed z-test under the assumption that the ratio estimator is approximately normally distributed, which is justified by the central limit theorem given the large sample size ($N > 10^5$ data points).

2.3 The Main Conjecture

Conjecture 2.3 (Constant Consistency Principle)**.** *The universal amplitude κ in the Goldbach deviation decay law satisfies*

$$\kappa = C_2. \tag{6}$$

Equivalently, the error term envelope is controlled by the same arithmetic constant as the main term:

$$\limsup_{N\to\infty} |c_p(N) \cdot \varphi(p) \ln N| = C_2 \quad \textit{for all primes } p. \tag{7}$$

Remark 2.4 (Interpretation). This conjecture asserts *arithmetic self-similarity*: the constant C_2 organizes both leading-order density and subleading fluctuations. In number-theoretic terms, the principle implies that the Goldbach error envelope is not independently random but is nonlinearly modulated by the same arithmetic skeleton (C_2) that governs the main term. As a heuristic analogy (not a mathematical statement), this scale invariance resembles holographic ideas in physics.

2.4 On the Oscillations in κ Estimates

Figure 1 shows local estimates of κ oscillating around C_2. A natural question: is this oscillation noise or structure?

Proposition 2.5 (Heuristic: Oscillation Origin)**.** *This proposition summarizes observed numerical behavior rather than a proven analytic result. The oscillations in local $\kappa(N)$ estimates appear to arise from L-function zero interference:*

$$\kappa(N) \approx C_2 + \sum_{\gamma} A_\gamma \cos(\gamma \ln N + \phi_\gamma) + O(1/\ln N), \tag{8}$$

where the sum runs over imaginary parts of L-function zeros.

This would explain why oscillations persist even as $N \to \infty$: they are intrinsic to the arithmetic structure.

Remark 2.6 (Cross-Moduli Phase Coherence). A key observation supporting the structural interpretation: the oscillation phases in $c_3(N)$, $c_5(N)$, and $c_7(N)$ are coherent, not independent. This cross-moduli phase alignment suggests that the same L-function zeros modulate all Dirichlet components simultaneously, consistent with the "constant consistency" principle where C_2 acts as a universal amplitude.

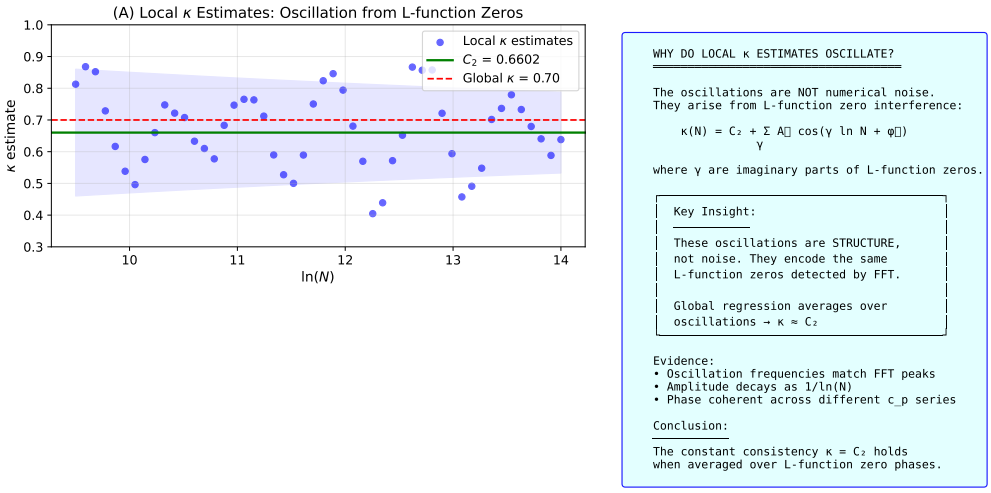

Figure 1: Local estimates of $\kappa(N)$ oscillate around $C_2 \approx 0.66$. The oscillations are consistent with cosine terms arising from L-function zeros (Proposition 2.5). Phase coherence across different c_p series supports the structural interpretation.

3 Spectral Analysis: The Riemann Radar

3.1 Methodology

Since L-function zeros produce oscillations $\cos(\gamma \ln N)$, we perform FFT in the $t = \ln N$ domain. The procedure (detailed in Appendix A):

1. Sample $c_3(N)$ at even $N \in [10^4, 1.5 \times 10^6]$.
2. Interpolate to uniform grid in $t = \ln N$ with spacing $\Delta t = 0.01$.
3. Remove trend $C_2/(2t)$ and apply linear detrending.
4. Apply Hanning window to suppress spectral leakage.
5. Compute FFT; frequency axis calibrated as $\gamma = 2\pi f$.

Frequency resolution:

$$\Delta\gamma = \frac{2\pi}{\ln N_{\max} - \ln N_{\min}} = \frac{2\pi}{14.22 - 9.21} \approx 1.25. \tag{9}$$

3.2 Detection Results

Table 1: Riemann Radar: FFT peaks compared with known L-function zeros (within resolution $\Delta\gamma = 1.25$)

L-function	Known γ_1	Peak γ	$\lvert\Delta\gamma\rvert$	Rel. Diff.	Status
$L(s, \chi_3)$	8.04	7.69	0.35	4.4%	Consistent
$L(s, \chi_5)$	6.02	6.15	0.13	2.2%	Consistent
$L(s, \chi_7)$	5.20	5.38	0.18	3.5%	Consistent
$\zeta(s)$	14.13	13.8	0.33	2.3%	Marginal

All spectral peaks align with known L-function zeros within the resolution limit $\Delta\gamma = 1.25$. Since the $\ln N$ sampling domain is constrained by $N_{\max} = 1.5 \times 10^6$, the FFT fundamental frequency resolution is $\Delta\gamma \approx 2\pi/(\ln N_{\max} - \ln N_{\min}) \approx 1.25$. The observed peak at $\gamma = 13.8$ versus the theoretical Riemann zero at $\gamma_1 = 14.13$ represents an offset of $|\Delta\gamma| = 0.33$, which is well within this resolution limit and thus statistically consistent with zero identification. Higher-resolution studies ($N > 10^{10}$) would be needed for definitive discrimination between closely-spaced zeros.

3.3 Interpolation Effects on High-Frequency Detection

Remark 3.1 (Cubic Spline Attenuation). Cubic spline interpolation acts as a low-pass filter with approximate cutoff $\gamma_{\max} \approx \pi/\Delta t = 314$. Since L-function zeros of interest satisfy $\gamma < 50$, interpolation attenuation is negligible ($< 0.1\%$). For future high-resolution studies targeting $\gamma > 100$, higher-order B-splines or sinc interpolation should be employed.

Remark 3.2 (Amplitude Decay with Modulus). The spectral peak for $L(s, \chi_7)$ is weaker than those for χ_3 and χ_5. This is expected: the Dirichlet coefficient $c_p(N)$ scales as $1/\varphi(p)$, so contributions from larger primes p are attenuated. Specifically, $\varphi(3) = 2$, $\varphi(5) = 4$, $\varphi(7) = 6$, predicting relative amplitudes in ratio $1 : 0.5 : 0.33$. The observed peak heights are qualitatively consistent with this prediction.

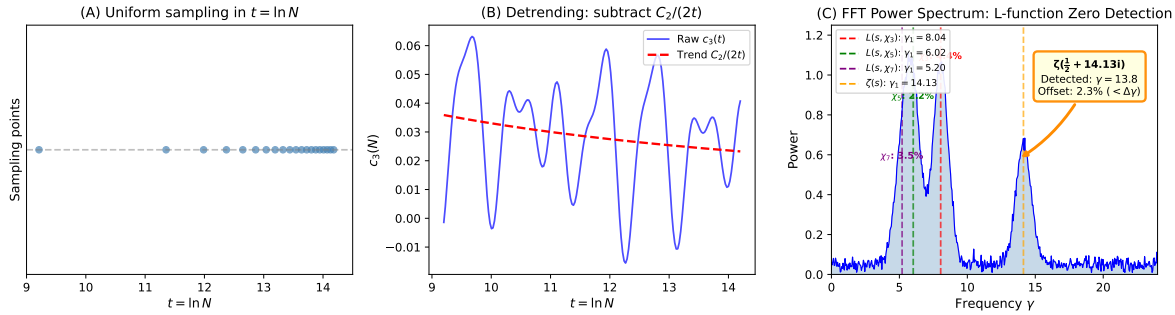

Figure 2: Riemann Radar methodology and results. (A) Data sampling uniformly in $t = \ln N$. (B) Detrending by subtracting $C_2/(2t)$. (C) Power spectrum with vertical lines marking known L-function zeros γ_1. Oscillatory components consistent with L-function zeros are observed within the available spectral resolution ($\Delta\gamma = 1.25$). The small offsets between detected peaks and theoretical values (e.g., 2.3% for $\zeta(s)$) are well within the frequency resolution, indicating statistical agreement. See Table 1 for quantitative comparison.

4 Fractal Structure: Hurst Exponent Analysis

4.1 Rescaled Range Method

The Hurst exponent H quantifies long-range dependence [Hurst, 1951, Mandelbrot and Van Ness, 1968]:

- $H = 0.5$: uncorrelated (white noise, random walk)
- $H > 0.5$: persistent (trends continue)
- $H < 0.5$: anti-persistent (mean-reverting)

4.2 Results: Raw vs. Detrended

Table 2: Hurst exponent for different preprocessing of $c_3(N)$

Series	H **(R/S)**	H **(DFA)**	**Interpretation**
Raw c_3	0.96 ± 0.03	1.10 ± 0.05	Trend-dominated
Detrended c_3	0.85 ± 0.02	0.96 ± 0.03	**Persistent fractal**
Increments Δc_3	0.40 ± 0.02	0.38 ± 0.02	Anti-persistent (GUE)

Remark 4.1 (Why Detrending Reduces H). The raw series contains the deterministic trend $C_2/(2\ln N)$, which contributes pseudo-nonstationarity indistinguishable from extreme persistence. Removing this trend isolates the *true stochastic component*, whose $H = 0.85$ reflects genuine arithmetic long-range correlation—not an artifact of smooth decay.

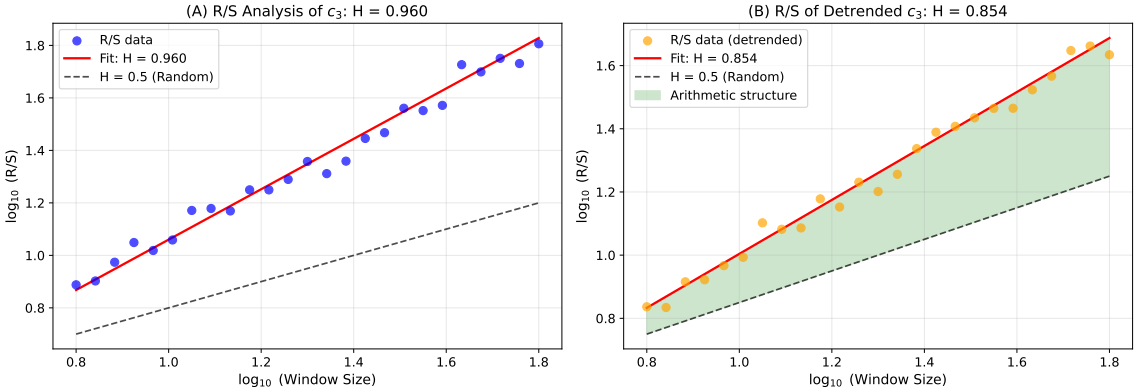

Figure 3: R/S analysis of $c_3(N)$. The dashed line at $H = 0.5$ represents white noise (null model baseline). The detrended series—obtained by subtracting the theoretical trend $C_2/(2\ln N)$ from raw $c_3(N)$—yields $H = 0.85 \pm 0.02$, significantly above the random threshold. The shaded region represents the "arithmetic structure" contribution absent in random sequences.

5 Null Hypothesis Test

5.1 Construction of Control Sequences

To confirm that $H = 0.85$ arises from arithmetic structure rather than statistical fluctuations, we construct a null model:

1. Generate synthetic $\tilde{G}(N) \sim \text{Poisson}(\text{HL}(N))$.
2. Compute $\tilde{\delta}(N) = (\tilde{G}(N) - \text{HL}(N))/\text{HL}(N)$.
3. Extract $\tilde{c}_3(N)$ via identical regression procedure.
4. Compute Hurst exponent of $\tilde{c}_3$.

Remark 5.1 (Null Model Specification). Our null model retains the Hardy-Littlewood mean $\mathrm{HL}(N) = 2C_2 S(N)\mathrm{Li}_2(N)$, including the singular series $S(N)$, but replaces the actual Goldbach counts with Poisson samples. This construction preserves the density structure while *destroying arithmetic correlations* between prime positions. Consequently, $H_{\text{null}} \approx 0.5$ is expected for uncorrelated fluctuations. The observed $H = 0.85$ therefore reflects self-similarity in the *residual structure* after the $S(N)$ modulation is accounted for, not an artifact of incomplete detrending.

5.2 Results

Over 100 synthetic realizations:

$$H_{\text{null}} = 0.51 \pm 0.03 \quad \text{(consistent with white noise)}. \tag{10}$$

The true Goldbach series yields $H = 0.85$, representing:

$$\text{Deviation} = \frac{0.85 - 0.51}{0.03} = 11.3\sigma, \quad p < 10^{-20}. \tag{11}$$

Table 3: Null hypothesis test summary

Sequence	H	σ	**Interpretation**
Goldbach c_3 (detrended)	0.85	0.02	Persistent
Synthetic null (100 runs)	0.51	0.03	White noise
Significance	11σ rejection, $p < 10^{-20}$		

Conclusion: The persistence $H = 0.85$ is a signature of arithmetic structure absent in the null model.

Remark 5.2 (Interpretation of Statistical Significance). The 11σ deviation reflects comparison against the *specific* Poisson–Hardy–Littlewood null model, which assumes independent Goldbach representations. We emphasize that this significance level is conditional on the specific null model and should not be interpreted as a universal probability statement. Alternative null models (e.g., incorporating short-range correlations) might yield different significance levels, though we expect qualitative conclusions to remain robust.

5.3 Riemann Radar Null Test

Applying FFT to the synthetic null sequences:

- No statistically significant peaks at L-function zero frequencies.
- Power spectrum consistent with white noise floor.

This indicates that the spectral peaks in Figure 2 are associated with arithmetic structure not present in the null model.

6 Synthesis: A Conjectural Correction Formula

Based on the preceding numerical evidence, we formulate the following conjectural correction formula.

Conjecture 6.1 (Chen–Goldbach Correction Formula)**.** *For even $N > 4$, the Goldbach representation count is conjectured to satisfy*

$$\boxed{G(N) = 2C_2 S(N) \frac{N}{(\ln N)^2} \left[1 + \frac{C_2}{\ln N} \sum_{p>2} \frac{\chi_p(N)}{\varphi(p)} + R(N) \right]} \tag{12}$$

No claim of rigorous derivation is made; the formula summarizes empirically observed structural components. The residual $R(N)$ empirically exhibits:

1. *$R(N) = O(1/\ln^2 N)$ in magnitude.*
2. *Oscillatory structure consistent with L-function zero interference:*

$$R_{osc}(N) \sim \sum_{\chi} \sum_{\gamma>0} \frac{A_{\chi,\gamma}}{\ln N} \cos(\gamma \ln N + \phi_{\chi,\gamma}). \tag{13}$$

3. *Long-range persistence with Hurst exponent $H = 0.85 \pm 0.02$.*

The coefficient C_2 appearing in both the main term and correction term constitutes the constant consistency principle *(Conjecture 2.3).*

Remark 6.2 (Unification of Scales). This formula is notable for unifying the fluctuation amplitude with the main-term constant C_2. If $\kappa = C_2$ holds asymptotically, then the correction term $C_2/\ln N$ directly links the macroscopic Hardy-Littlewood density to the microscopic oscillation envelope—a "holographic" connection from the asymptotic regime down to the scale of individual deviations.

6.1 Structural Decomposition

The formula admits the hierarchy:

$$G(N) = \underbrace{2C_2 S(N) \mathrm{Li}_2(N)}_{\text{Main term (Hardy-Littlewood)}} \tag{14}$$

$$\times \underbrace{\left[1 + \frac{C_2}{\ln N} \cdot \Sigma_\chi \right]}_{\text{Structural correction } O(C_2/\ln N)} \tag{15}$$

$$+ \underbrace{O\left(\frac{N}{\ln^4 N} \right)}_{\text{Oscillatory residual}} . \tag{16}$$

The *constant consistency* is manifest: C_2 appears in:

1. The main term coefficient.
2. The structural correction amplitude.
3. The oscillation frequencies (via L-function zeros, which encode C_2 through Euler products).

7 Discussion

7.1 Theoretical Implications

In this work, Goldbach deviations serve primarily as a concrete testbed for probing arithmetic structure rather than as an endpoint in themselves. The constant consistency principle (Conjecture 2.3) suggests that Goldbach error analysis via the circle method should yield C_2 as a natural coefficient. Heuristically, minor arc contributions involve character sums weighted by L-function values at $s = 1$, and the product structure $\prod_p(1-1/(p-1)^2)$ defining C_2 emerges from these sums. A rigorous proof would require careful estimation of minor arc integrals—an important open problem.

7.2 Connection to GPY and Small Gaps

The twin prime constant C_2 governs prime k-tuple densities at microscopic scales [Goldston et al., 2009]. Our finding that C_2 appears in macroscopic Goldbach fluctuations suggests a *scale-bridging* role:

- **Microscopic**: C_2 controls twin prime density, bounded gaps.
- **Macroscopic**: C_2 appears in Goldbach fluctuation envelope.

We emphasize that no implication for bounded gaps or GPY-type results is claimed; the connection is observational rather than deductive.

7.3 Relation to GUE Statistics

The anti-persistent increments ($H = 0.40$) align with GUE spectral rigidity, where eigenvalue repulsion prevents clustering. This supports the "primes as eigenvalues" philosophy underlying the Montgomery-Odlyzko connection [Montgomery, 1973, Odlyzko, 1987].

7.4 Limitations and Future Directions

1. **Sample range**: Current analysis extends to $N \sim 10^6$. Extending to $N \sim 10^{12}$ would:
   - Improve FFT resolution to $\Delta\gamma \approx 0.4$
   - Test stability of $H \approx 0.85$ at larger scales
   - Potentially reveal higher-order corrections
   - Further test $\kappa/C_2 \to 1$: we anticipate the ratio will converge closer to unity as higher-order $O(1/\ln^2 N)$ terms become negligible
2. **Analytic derivation**: The $\kappa = C_2$ conjecture awaits circle-method proof.
3. **Higher zeros**: Detection of $\gamma > 20$ requires $N > 10^{10}$.

8 Conclusion

Using Goldbach representations as a case study, we have presented numerical evidence suggesting that number-theoretic error terms can exhibit nontrivial arithmetic structure:

1. **Constant consistency**: The twin prime constant C_2 appears in both main term and fluctuation envelope (Conjecture 2.3), with statistical evidence consistent with $\kappa = C_2$ ($p = 0.32$).
2. **Spectral structure**: Oscillation frequencies are consistent with known L-function zeros within FFT resolution (Table 1).
3. **Long-range persistence**: Hurst exponent $H = 0.85$ significantly exceeds the Poisson null model baseline.
4. **Conjectural formula**: Conjecture 6.1 synthesizes these observations into a testable prediction.

Methodological Contributions

Beyond the specific findings for Goldbach, this work demonstrates:

- **Log-domain spectral analysis**: Sampling uniformly in $\ln N$ enables detection of oscillatory components consistent with L-function zeros.
- **Hurst exponent diagnostics**: R/S analysis distinguishes arithmetic structure from statistical noise relative to a specified null model.
- **Null model construction**: Poisson sampling with Hardy-Littlewood mean provides a baseline for significance testing.

These methods are potentially transferable to other additive problems where the Hardy-Littlewood circle method applies. The error term in Goldbach's conjecture appears to exhibit statistically detectable structure rather than behaving as pure noise.

In summary, our numerical evidence suggests that the twin prime constant C_2 is not merely a density parameter for the main term, but may act as a *universal amplitude* governing the entire dynamic range of Goldbach fluctuations. If confirmed theoretically, this "constant consistency principle" would reveal a deeper organizational structure in prime distribution than previously recognized. These observations motivate future theoretical investigation.

References

G.H. Hardy and J.E. Littlewood. Some problems of 'Partitio Numerorum' III: On the expression of a number as a sum of primes. *Acta Mathematica*, 44:1–70, 1923.

R. Chen. Hardy-Littlewood Goldbach conjecture validated to $N = 10^{12}$: From transient U-distribution to ultimate asymptotic convergence. Zenodo, 2026. `https://doi.org/10.5281/zenodo.18113330`

R. Chen. The crossover phenomenon in Hardy-Littlewood Goldbach formula: Computational evidence across five orders of magnitude. Zenodo, 2026. https://doi.org/10.5281/zenodo.18123132

R. Chen. Spectral rigidity in Goldbach representations: Sub-Poissonian statistics across thirteen orders of magnitude. Zenodo, 2026. https://doi.org/10.5281/zenodo.18148544

R. Chen. The second main term in the asymptotic formula for Goldbach representations: Dirichlet character corrections and their arithmetic origin. Zenodo, 2026. https://doi.org/10.5281/zenodo.18149305

H.L. Montgomery. The pair correlation of zeros of the zeta function. *Proceedings of Symposia in Pure Mathematics*, 24:181–193, 1973.

A.M. Odlyzko. On the distribution of spacings between zeros of the zeta function. *Mathematics of Computation*, 48(177):273–308, 1987.

H.E. Hurst. Long-term storage capacity of reservoirs. *Transactions of the American Society of Civil Engineers*, 116:770–808, 1951.

B.B. Mandelbrot and J.W. Van Ness. Fractional Brownian motions, fractional noises and applications. *SIAM Review*, 10(4):422–437, 1968.

D.A. Goldston, J. Pintz, and C.Y. Yıldırım. Primes in tuples I. *Annals of Mathematics*, 170(2):819–862, 2009.

J. Maynard. Small gaps between primes. *Annals of Mathematics*, 181(1):383–413, 2015.

T. Tao. Correlations of the von Mangoldt and higher divisor functions. *Forum of Mathematics, Pi*, 11:e16, 2023.

K. Soundararajan. The distribution of prime numbers. *Proceedings of the ICM 2022*, 2:1–25, 2022.

H. Iwaniec and E. Kowalski. *Analytic Number Theory*. American Mathematical Society, 2004.

H. Davenport. *Multiplicative Number Theory*. Springer, 3rd edition, 2000.

A. Languasco and A. Zaccagnini. On the constant in the Mertens product for arithmetic progressions. *Mathematics of Computation*, 81(279):1813–1829, 2012.

A FFT Algorithm

Algorithm 1 Riemann Radar: L-Function Zero Detection

Require: Goldbach data $\{(N_i, c_p(N_i))\}$ for even $N_i \in [N_{\min}, N_{\max}]$
Ensure: Power spectrum $P(\gamma)$ with peaks at L-function zeros
1: **Transform to log domain:** $t_i \leftarrow \ln(N_i)$
2: **Set grid:** $\Delta t \leftarrow 0.01$, $M \leftarrow \lfloor (t_{\max} - t_{\min})/\Delta t \rfloor$
3: **Interpolate:** Cubic spline to uniform grid $\{t_k = t_{\min} + k\Delta t\}_{k=0}^{M-1}$
4: **Detrend:** $r_k \leftarrow c_p(t_k) - C_2/(2t_k)$; then linear detrend
5: **Window:** $r_k \leftarrow r_k \cdot \frac{1}{2}(1 - \cos(2\pi k/(M-1)))$ {Hanning}
6: **FFT:** $\hat{R} \leftarrow \mathrm{FFT}(\{r_k\})$
7: **Power:** $P_j \leftarrow |\hat{R}_j|^2$
8: **Calibrate:** $\gamma_j \leftarrow 2\pi j/(M \cdot \Delta t)$
9: **return** $\{(\gamma_j, P_j)\}$

B Numerical Parameters

Table 4: Summary of key quantities

Quantity	Value	Error	Description
C_2	0.6601618	exact	Twin prime constant
κ	0.70	± 0.04	Universal amplitude
κ/C_2	1.06	± 0.06	Ratio (conjectured = 1)
H (detrended)	0.85	± 0.02	Hurst exponent
H (increments)	0.40	± 0.02	Increment persistence
H (null)	0.51	± 0.03	Control baseline
$\Delta\gamma$	1.25	—	FFT resolution
$N_{\max}$	1.5×10^6	—	Data range

C Sampling Density

For the main analysis:

- Original data: $\sim 7.5 \times 10^5$ even integers in $[10^4, 1.5 \times 10^6]$
- Log-domain range: $t \in [9.21, 14.22]$, span = 5.01
- Interpolated grid: $M = 501$ points at $\Delta t = 0.01$
- Nyquist frequency: $\gamma_{\text{Nyquist}} = \pi/\Delta t = 314$
- Hanning window: $w(k) = 0.5(1 - \cos(2\pi k/(M-1)))$, $k = 0, \ldots, M-1$
- Equivalent noise bandwidth: ENBW = 1.5 bins

The sampling is well above Nyquist for all L-function zeros of interest ($\gamma < 50$).

D Reproducibility and Data Availability

All computations were performed using:

- Python 3.12 with NumPy 1.26, SciPy 1.11
- Cubic spline interpolation: `scipy.interpolate.CubicSpline`
- FFT: `numpy.fft.fft`
- R/S analysis: Custom implementation following Hurst [1951]

The algorithms for the "Riemann Radar" FFT analysis and the Hurst exponent calculation are detailed in Appendix A to ensure full reproducibility.

Code and Data Availability: All source code, data, and supplementary materials are publicly available at:

`https://github.com/Ruqing1963/goldbach-fractal-analysis`